Field-controlled adhesion in confined magnetorheological fluids

Sérgio A. Lira and José A. Miranda*
Departamento de Física, LFTC, Universidade Federal de Pernambuco, Recife 50670-901, PE, Brazil
(Received 10 June 2009; published 20 October 2009)

The study of reversible, functional, and controllable adhesives is a matter of considerable practical interest, and academic research. We report the adhesive response of a magnetorheological fluid confined between two parallel plates under a probe-tack test, when it is subjected to an applied magnetic field. Our analytical approach is based on a Darcy-like law formulation which considers a magnetic field-dependent yield stress behavior. The adhesion force is calculated in closed form for two different configurations produced by a Helmholtz coils setup: uniform perpendicular, and nonuniform radial magnetic fields. In both cases, we verify that adhesion force is hugely increased as a result of the field-dependent nature of the yield stress. This provides a versatile way to obtain a shear resistant, tough structural adhesive through magnetic means.

DOI: 10.1103/PhysRevE.80.046313 PACS number(s): 47.65.Cb, 47.57.Qk, 68.35.Np, 83.60.La

I. INTRODUCTION

During the last few years there has been a continuous interest in the study of the adhesion properties of fluids [1–12]. These investigations have scrutinized, both theoretically and experimentally, a variety of situations involving Newtonian, non-Newtonian (shear-thinning, shear-thickening, viscoelastic, etc.), and magnetic fluids (ferrofluids and magnetorheological fluids). A common goal in all these studies was to measure and evaluate the adhesive performance of a given fluid material through the so-called probe-tack test [13,14]. In the plate-plate variant of this test, a fluid sample is confined between two parallel plane plates, and then the upper plate is lifted vertically at a known rate. In response to this confined shearing flow a downward adhesive force normal to the upper plate is produced and properly recorded. This quantifies the adhesive strength of the fluid sample under tension as a function of the upper plate displacement.

One very important aspect in adhesion science and in its applications is the ability to control the bond strength of adhesives. With respect to this point, a suggestive control mechanism has been proposed in Ref. [7], which investigated adhesion phenomena in viscous, *Newtonian* ferrofluids. Ferrofluids [15,16] are stable colloidal suspensions of nanometersized magnetic particles suspended in a nonmagnetic carrier fluid. These magnetic fluids behave superparamagnetically and can easily be manipulated with external magnetic fields. It has been shown that the adhesive properties of a ferrofluid can be enhanced or reduced by varying the intensity, and geometric configuration of an externally applied magnetic field [7]. Within this context, a ferrofluid would act as a sort of adjustable "magnetic glue" for which the adhesion strength is regulated by magnetic means.

Most conventional adhesives are based on weakly crossed-linked high-molecular weight polymers, so usually they are markedly non-Newtonian, and present very complex rheological properties. In order to conciliate the complicated non-Newtonian aspects of regular adhesive materials, and the magnetically controlled adhesion mechanism offered by magnetic fluids, the adhesion properties of *non-Newtonian*, chain forming ferrofluids have been examined [12]. The development of denser and more strongly magnetized ferrofluids has revealed a wide range of non-Newtonian behaviors in these liquids [17,18], which are attributed to the formation of short chains when the magnetic particles are exposed to strong magnetic fields. The results obtained in Ref. [12]. indicate that the existence of these short chains has a significant impact on the adhesive strength as well as on the viscosity of the ferrofluid, making it to display both shear-thinning and shear-thickening regimes. This opened up the possibility of monitoring complex rheological responses of such fluids with the assistance of applied magnetic fields.

Despite the stimulating magnetic field-induced adhesive properties displayed by both Newtonian [7] and non-Newtonian [12] ferrofluids, key effects like viscoelasticity and plasticity, which are common in ordinary adhesives, seem not to be present in such magnetic fluids. These effects are very important if one needs to increase the adhesion strength between surfaces, where a shear resistant, tough structural adhesive is necessary. As a matter of fact, the possible appearance of viscoelastic properties such as yield stress in ferrofluids, and its dependence on the applied magnetic field has been recently investigated experimentally [19,20]. Note that as opposed to Newtonian fluids, yield stress fluids [21] can support shear stresses without flowing. As long as the stress remains below to a certain critical value they do not flow, but respond elastically to deformation. It has been shown that in ferrofluids the yield stress is proportional to the square of the applied magnetic field strength. But, unfortunately, it has also been found that the field-dependent yield stress is very small [$O(10^{-2}$ Pa-10^{-1} Pa)]. Therefore, one should not expect a dramatic change in the yield stress properties of existing ferrofluids by applying a magnetic field.

In contrast to ferrofluids which present particles with diameters of a few nanometers, magnetorheological (MR) fluids typically consist of micronsized magnetized particles dispersed in aqueous or organic carrier liquids. The unique feature of this type of magnetic fluid is the abrupt change in its viscoelastic properties upon the application of an external magnetic field [22–26]. The changes are significant

*jme@df.ufpe.br

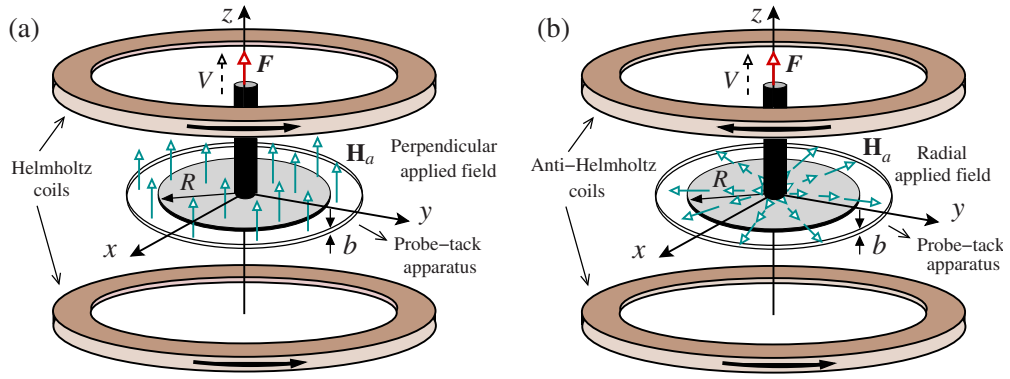

FIG. 1. (Color online) Schematic representation of the probe-tack apparatus, where a circular MR fluid drop of radius R and thickness b is confined between parallel plates, and subjected to (a) a perpendicular and (b) a radial magnetic field configuration. The direction of the electric currents flowing in the coils is also indicated. The upper plate is lifted at constant velocity V through the application of a force F. The lower plate remains at rest located at the mid-plane between the coils (x-y plane).

$[O(10^5-10^6)]$, occur within a few milliseconds, and are nearly completely reversible. In the absence of an applied field ("off" state) the magnetized particles in the suspension are randomly distributed, so that MR fluids appear similar to liquids paints, exhibiting comparable levels of apparent viscosity. When a magnetic field is applied ("on" state) the particles suspended in the fluid interact, and tend to align and link together along the field's direction, creating long particle chains, columns, and other more complex structures. The formation of such structures restricts the motion of the fluid, causing it to display a solidlike behavior.

The efficiency of a MR fluid can be evaluated by its yield stress, which measures the strength of the field-induced structures formed. This yield stress increases as the magnitude of the applied magnetic field is increased, and is associated to the highest value of stress (for which no flow is observed) required to break the existing network of magnetic interactions. In this sense, MR fluids work as smart liquid materials whose viscoelastic properties can be conveniently tuned by an applied magnetic field. This suggests that the potential of external magnetic fields in providing controllable changes in the adhesion performance and structural toughness of magnetic fluids as originally proposed in Refs. [7,12] has not been exhausted. In the case of MR fluids, this possibility has been recently investigated by an experimental group from MIT led by Hosoi and McKinley [11] who conducted probe-tack experiments using a MR fluid subjected to an inhomogeneous magnetic field produced by a small cylindrical magnet. Their experiments revealed orders of magnitude difference in the adhesion properties of the MR fluid when the magnetic field is applied [11]. It has also been found that the yield stress depends quadratically on the strength of the applied field. Despite these promising news, a systematic theoretical study of the adhesion phenomena in confined MR fluids under probe-tack test circumstances still needs to be undertaken. This is the main purpose of this work.

In this paper we study the adhesion properties of a confined MR fluid, subjected to two distinct magnetic field configurations as sketched in Fig. 1: (a) perpendicular, when the applied field is uniform and acts perpendicular to the plates of the probe-tack apparatus; and (b) radial, for a radially increasing in-plane field which is tangential to the plates. This allows us to examine how the adhesive strength of the MR fluid depends on the mutual orientation of the magnetic field and the direction of deformation. Under such circumstances, the combined influence of the magnetic field arrangement and the field-dependent yield stress in determining the adhesive response of the fluid is studied analytically. The bond strength obtained for the general situation involving both magnetic field and field-induced yield stress is contrasted with the responses of other two important scenarios in which, first, there is no applied magnetic field (yield stress fluid, but effectively nonmagnetic), and then the magnetic field is applied, but the fluid is assumed to be of low yield stress (fluid is magnetic, but of negligible field-induced yield stress). In summary, the purpose of our work is to study the coupling between field-induced structuring and hydrodynamic interactions, and examine their role in providing a control of the adhesive strength of MR fluids by means of applied magnetic fields.

II. CALCULATION OF THE ADHESION FORCE: DARCY-LIKE LAW APPROACH

Figure 1 sketches the geometry of the system. We consider a MR fluid confined between two narrowly spaced circular, flat plates. One end of the lifting apparatus, connected to the upper plate, moves at a specified constant velocity V, subjecting this plate to a pulling force $\mathbf{F}=F\,\hat{\mathbf{z}}$, where $\hat{\mathbf{z}}$ is the unit vector along the z-axis. We consider that the apparatus has a spring constant k, and that the lower plate is held fixed at $z=0$. The initial plate-plate separation is represented by b_0, and the initial radius of the fluid drop is denoted by R_0. At a given time t the plate spacing is given by $b=b_0+Vt$, where $V=\dot{b}=db/dt$.

The confined MR fluid is subjected to two different magnetic field configurations (Fig. 1), both produced by a pair of current-carrying coils such that the applied field is (a) uniform and perpendicular or (b) radially increasing and coplanar with the lower plate. The coils are mounted so they are parallel to (and coaxial with) the plates. Note that these two distinct magnetic field configurations can be conveniently

obtained by using a single magnetic coils arrangement, the only difference being the relative direction of the electric currents flowing in the coils.

Our aim is to calculate the pulling force F analytically as a function of the upper plate displacement b, by taking into account the viscoelastic and magnetic nature of the yield stress MR fluid. As shown in Ref. [2] the compliance of the lifting apparatus can be safely neglected. Moreover, we follow Refs. [2–9] and derive F assuming that the border of the MR fluid drop remains circular during the entire lifting process, with time-dependent radius defined as $R=R(t)$. Conservation of fluid volume leads to the relation $R^2b=R_0^2b_0$.

Within the framework of the lubrication approximation, where the distance between the plates b is much smaller than the radius R of the fluid drop, and by neglecting inertial effects, a Darcy-like law for a yield stress fluid can be written as [27–30]

$$\frac{dp}{dr} = \frac{2\sigma_y}{b}[1 + f(\dot{\gamma})], \tag{1}$$

where p is the gap-averaged hydrodynamic pressure, σ_y is the yield stress, $\dot{\gamma} \sim V/b$ denotes the shear rate, and the function $f(\dot{\gamma})$ includes viscous contributions and tends to zero when $\dot{\gamma} \to 0$.

By assuming a low shear regime, taking into account the contribution of magnetic forces, and the existence of a magnetic field-dependent yield stress $\sigma_y = \sigma_y(H)$, we rewrite Eq. (1) as a modified Darcy's law for confined MR fluids

$$\frac{d\Pi}{dr} = \frac{2\sigma_y(H)}{b}, \tag{2}$$

where

$$\Pi = \frac{1}{b}\int_0^b [p - \Psi]dz \tag{3}$$

is a gap-averaged generalized pressure in which

$$\Psi = \mu_0 \int_0^H M dH \tag{4}$$

denotes a magnetic pressure, where μ_0 denotes the magnetic permeability of free space, and M is the magnetization of the MR fluid. In this context, the magnetic body force acting on the MR fluid is given by $\mu_0 M \nabla H$ [15,16], where H is the local magnetic field. The low shear rate limit ($\dot{\gamma} \to 0$) is justified by the fact that in probe-tack experiments $\dot{\gamma}$ is usually very low [2,4,5,9]. The replacement of p by the generalized pressure Π is also a standard procedure in the study of confined magnetic fluid flow problems [31,32].

On the basis of the experimental findings of Refs. [11,19,20] and in agreement with the theoretical models discussed in Refs. [24–26], we assume the following relation between the yield stress and the local magnetic field H,

$$\sigma_y(H) = \sigma_{y0} + \alpha H^2, \tag{5}$$

where σ_{y0} represents the yield stress in the absence of the magnetic field, and α is a constant that depends on the material properties of the MR fluid, being proportional to the particle volume fraction [26]. In general the field dependence of a yield stress fluid is represented by a power law $\sigma_y(H) \sim H^n$ with $1 \le n \le 2$, and the case we consider here $n=2$ is the one for which the magnetization is linearly related to the applied magnetic field [24–26] $\mathbf{M} = \chi \mathbf{H_a}$, where χ is the magnetic susceptibility. This linear relation holds as long as $H_a \ll H_{sat}$, where H_{sat} is the field magnitude at saturation magnetization [$O(10^2$ kA/m-10^3 kA/m)].

The local magnetic field can include contributions from the applied field as well as the demagnetizing field. We consider only the lowest-order effect of the magnetic interactions [33]. Thus, in the perpendicular situation, we include the demagnetizing field produced by the uniform magnetization resulting from the applied field. However, in the radial field case, we consider only the action of the applied field, and neglect demagnetazing effects. Despite the similarity of these assumptions with the ones considered for the case of ferrofluids [7], we stress that the Darcy's law form given by Eq. (2) and the existence of a sizable magnetic field-dependent yield stress as expressed by Eq. (5) are unique features of MR fluids.

The force exerted by the lifting apparatus on the upper plate is calculated by integrating the hydrodynamic pressure difference above and below it [7,12], yielding

$$F = \int_0^R 2\pi r dr \left\{ [\Pi(R) - \Pi(r)] + [\Psi(R) - \Psi(r)] + \frac{1}{2}\mu_0[M_r^2(R) - M_z^2(r)] \right\}. \tag{6}$$

Notice that the first term inside the curly brackets is readily calculated by integrating Eq. (2). On the other hand, the terms $M_r(R)$ and $M_z(r)$ denote the normal component of the magnetization evaluated at the boundaries $r=R$, and $z=b$, respectively. These terms derive from the pressure jump boundary condition [15,16]

$$\Delta p = -\frac{1}{2}\mu_0 M_n^2, \tag{7}$$

where as in Refs. [2,9] we have neglected surface-tension effects. In Eq. (7), M_n represents the normal component of the magnetization at the fluid boundaries.

III. TWO FIELD CONFIGURATIONS: RESULTS AND DISCUSSION

In this section we calculate closed-form expressions for the adhesion force [Eq. (6)] by considering that the applied magnetic field is perpendicular, or radially symmetric. For each case, we discuss how the force F varies as a function of the plate separation b for typical values of the dimensionless control parameters of the system. While presenting our results we make sure that the values of all relevant dimensionless quantities we utilize are consistent with realistic physical parameters related to existing probe-tack test instruments, magnetic field arrangements, and material properties of MR fluids. For the typical parameters related to probe-tack experiments we take [2,4,5,9]: $k=5.0\times10^5$ N/m, R_0

$=10^{-2}$ m, $b_0=10^{-4}-10^{-3}$ m, and $V=10^{-7}-10^{-6}$ m/s. While dealing with the strength of the magnetic fields, we consider relatively low values $5\leq H_0\leq 30$ kA/m which are easily achievable by using a typical Helmholtz coils setup, where the radius of a coil is considerably larger than the radius of the MR fluid droplet. The characteristic length L related to the radial magnetic configurations is of the order of a few centimeters [34]. It is also worth pointing out that the plate dimensions of real probe-tack apparatus and the size of the magnetic coils are compatible. Regarding the material properties of the MR fluid we take $\alpha=3.0\times10^{-7}$ N/A^2 [11,19] and consider that the "off" state yield stress σ_{y0} varies from 3 to 45 Pa [11,35]. Finally, for the magnetic susceptibility we take $0.1\leq\chi\leq1$ [36].

A. Perpendicular magnetic field

First, we consider the perpendicular field case in which a uniform magnetic field,

$$\mathbf{H}_a = H_0\hat{\mathbf{z}}, \tag{8}$$

is applied normal to the parallel plates of the probe-tack apparatus. In a laboratory this perpendicular field configuration can be readily generated by a pair of identical Helmholtz coils whose electric currents have the same magnitude and flow in the same direction. In consequence to its relatively easy practical implementation the perpendicular field arrangement has been largely utilized to investigate both experimentally and theoretically various aspects of the physics behind complex magnetic fluids.

Due to the demagnetizing effects [15,16], the uniformity of the perpendicular magnetic field is distorted inside the MR fluid sample. Our calculation takes such important effects into consideration in an explicit manner. By utilizing Eq. (4) and considering that the local magnetic field differs from the externally applied field by a droplet-shape-dependent demagnetizing field such that $\mathbf{H}=\mathbf{H_a}+\mathbf{H_d}$, where $\mathbf{H_d}=-\boldsymbol{\nabla}\varphi$, the magnetic pressure for the perpendicular field can be obtained. The magnetic potential φ arises from magnetic charges along the top and bottom surfaces of the circular fluid domain, and is equivalent to the one calculated for a parallel-plate capacitor [37].

By using Eqs. (3) and (4) we can describe the MR fluid boundary by a simple closed curve C parametrized by arclength s and rewrite the gap-averaged magnetic pressure as [7,31,32]

$$\Psi_\perp = \frac{\mu_0 M^2}{2\pi b}\left\{\oint_C ds'\hat{\mathbf{D}}\times\hat{\mathbf{t}}(s') + \oint_C dx'\,\ln[(y-y') + \sqrt{D^2+b^2}]\right\}, \tag{9}$$

where $x=x(s)$, $x'=x(s')$, etc., $\hat{\mathbf{t}}(s')$ is the unit tangent vector at arclength s', and $\hat{\mathbf{D}}=\mathbf{D}/D$ is the unit difference vector pointing from the point $\mathbf{r}=(x,y)$ to the point $\mathbf{r}'=(x',y')$. Substituting Eq. (9) into Eq. (6) results in a *dimensionless* adhesion force

$$F_\perp = \frac{1}{b^{5/2}}\left\{1+N_N^\perp\left[1-\frac{24\chi\beta}{\pi b^{3/2}}\int_0^1 udu\int_u^1 \mathcal{I}(u')du'\right]\right\} - N_B^\perp\frac{\chi^2}{b}\left[\frac{\pi}{2}-\frac{4\beta}{b^{3/2}}\left(\int_0^1 \mathcal{I}(u)udu-\frac{1}{2}\mathcal{I}(1)\right)\right], \tag{10}$$

where

$$\mathcal{I}(u) = \int_0^{\pi/2}\left(\frac{1-u+2u\,\sin^2\omega}{\sqrt{(1-u)^2+4u\,\sin^2\omega}}\right)d\omega + \frac{1}{2}\int_0^\pi \ln\left[\sqrt{1+(1-u)^2\frac{R^2}{b^2}+4\frac{R^2}{b^2}u\,\sin^2\omega} - \frac{R}{b}\sin 2\omega\right]\sin 2\omega d\omega. \tag{11}$$

$N_B^\perp=(\mu_0H_0^2R_0^2b_0)/k\zeta^2$ is the magnetic Bond number for the perpendicular magnetic field configuration, $N_N^\perp=\alpha H_0^2/\sigma_{y0}$ is the "non-Newtonian" dimensionless parameter which measures the relative strength of magnetically induced yield stress effects with respect to the "off" state yield stress. The parameter $\beta=(b_0^{1/2}R_0)/\zeta^{3/2}$ is a dimensionless geometric factor related to the demagnetizing field. Note that the adhesion force obtained in Eq. (10) has been rescaled by $k\zeta=(2\pi\sigma_{y0}R_0^3b_0^{3/2})/3\zeta^{5/2}$. In addition, lengths have been rescaled by ζ. This somewhat complex rescaling of the data has been originally introduced by the work of Derks *et al.* [2], where adhesion phenomena in nonmagnetic fluids have been studied both experimentally and theoretically. For consistency, and also to allow a more direct connection with Refs. [2,7,12] we adopted the same rescaling. We point out that, after appropriate reintroduction of dimensions, our adhesion force expression (10) agrees with the equivalent formula obtained in Refs. [2,28], which examined the considerably simpler case where the yield stress fluid is nonmagnetic ($N_B^\perp=N_N^\perp=0$).

Figure 2 plots the force-distance curves for the perpendicular field case, assuming that $\beta=3.16\times10^3$, $b_0=10$, and $\chi=0.1$. Figure 2(a) considers a fixed value of $N_B^\perp=0.15$ and three different values of $N_N^\perp$: 62.50 (light gray curve), 31.25 (medium gray curve) and 15.62 (dark gray curve). As expected, by inspecting Fig. 2(a) we verify that for a fixed value of $N_B^\perp$, the adhesion force becomes increasingly larger for higher values of the non-Newtonian parameter $N_N^\perp$. Recall that in practice the magnitude of $N_N^\perp$ can be tuned by varying the strength of the applied field (H_0), or by manipulating the magnetic properties of the MR fluid (α), namely, its particle volume fraction. This is exactly the type of control mechanism that can be used to either enhance or decrease the adhesion performance of a MR fluid by magnetic means.

A log-log plot of the force-distance curves is presented in Fig. 2(b) where the lifting of the upper plate occurs for three distinct situations: (i) field-dependent yield stress MR fluid under the influence of a perpendicular field ($N_N^\perp=62.50$ and $N_B^\perp=0.15$, solid gray curve); (ii) field-independent yield stress MR fluid under the influence of a perpendicular field ($N_N^\perp=0$ and $N_B^\perp=0.15$, solid black curve); and (iii) MR fluid

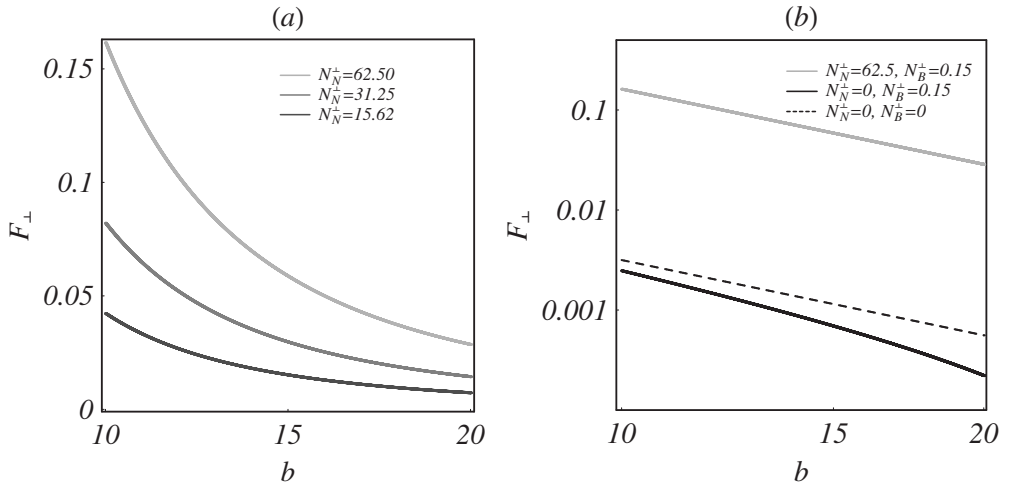

FIG. 2. Adhesion force for the perpendicular field case $F_\perp$ as a function of displacement b, for (a) $N_B^{\perp}=0.15$ and three values of $N_N^{\perp}$; and (b) contrasting the case of zero applied field (dashed curve), with the ones assuming the action of the perpendicular field, for a field-independent (solid black curve), and a field-dependent (solid gray curve) yield stress MR fluid. It is assumed that $\beta=3.16\times10^3$, $b_0=10$, and $\chi=0.1$.

in the absence of an applied magnetic field, or "off" state MR fluid ($N_N^{\perp}=0$, $N_B^{\perp}=0$, dashed curve). The first noteworthy aspect of this system is the decrease in adhesion force purely due to the magnetic field, i.e., when the field-dependent yield stress is negligible. This can be verified by observing that the solid black curve lies below the dashed one. We point out that the relative (minimum) difference between these two curves is on the order of 22%. This result indicates a real, potentially observable difference in behavior due to the magnetic field, since a shift in data as small as 20% is expected to be resolvable by current experimental techniques [38]. This behavior (decrease in $F_\perp$) for field-independent yield stress MR fluids is similar to the one detected in Ref. [7] for Newtonian ferrofluids subjected to a perpendicular field. Even though magnetic dipole-dipole repulsion tends to make the confined droplet to spread out (what would make the adhesion force to increase), the normal component of the magnetization acting on the upper plate has a more relevant role, and the net effect is a decrease in adhesion.

A completely different scenario is revealed when one considers the situation involving a field-dependent yield stress MR fluid [gray curve in Fig. 2(b)]. In this case one can verify a dramatic increase in $F_\perp$ with respect to the nonmagnetic situation (dashed curve). Notice that here the effect exclusively due to the magnetic field, which tends to diminish $F_\perp$, is completely obscured by the field-dependent yield stress contribution. In fact the adhesion force for the field-dependent yield stress MR fluid is about 50 times larger than the one calculated for the nonmagnetic case. Although an increase in the value of the adhesion force when one increases the yield stress is not really surprising, such an enormous field-induced magnification could not been trivially anticipated. We stress that this is a very significant increase in comparison with the usual responses computed for Newtonian (typical increase around 20–30%) [7] and non-Newtonian (increase of roughly 80%) [7] ferrofluids. This expressive change in the adhesion strength of the fluid material is due the formation of large particle chains, and the important dependence of its yield stress behavior on the magnetic field as expressed in Eq. (5). It is also worth noting that analogous order-of-magnitude difference has been observed experimentally in Ref. [11], where a field-dependent yield stress MR is subjected to the magnetic field of a small magnet.

We close our discussion about the perpendicular field case by adding a few remarks about Fig. 2(b). Up until this point we have focused our analysis on the magnitude of the adhesion force. Now we comment on the specific form of the force displacement curves, by addressing their dependence on the plate separation b. We begin by inspecting Eq. (10), and consider the zero applied field case ($N_N^{\perp}=N_B^{\perp}=0$) where $F_\perp \sim b^{-5/2}$ as represented by the dashed line. This is in agreement with the results originally obtained in Refs. [2,28] for nonmagnetic fluids. Another case of interest is the one related to the field-independent yield stress situation ($N_N^{\perp}\neq 0$ and $N_B^{\perp}\neq 0$) as depicted by the solid black curve. Under such circumstances, the demagnetizing term proportional to β contributes to an enhanced adhesion, and presents a nontrivial dependence on b, where a term proportional to $b^{-5/2}$ is multiplied by the complicated integral expression given by Eq. (11). On the other hand, the remaining term proportional to $N_B^{\perp}$ comes from the normal magnetization piece in Eq. (6), and scales as b^{-1}, acting to decrease the adhesion force. Since in Fig. 2(b) the solid black curve lies below the dashed one, we conclude that the normal magnetization term is prevalent. The net contribution of all the terms proportional to $N_B^{\perp}$ results in the following scaling: $\sim b^{-2.9}$ for smaller b, and $\sim b^{-4.7}$ for larger b.

Finally, we turn to the field-dependent yield stress case ($N_N^{\perp}\neq 0$, $N_B^{\perp}\neq 0$) related to the solid gray curve in Fig. 2(b). Now, the demagnetizing term proportional to $N_N^{\perp}$ and β tends to decrease the adhesion, presenting a complex dependence proportional to b^{-4} multiplied by the integral term. However, the dominant term is the one proportional to $N_N^{\perp}$, and independent of β which scales with $b^{-5/2}$. Note that this is the term that dramatically increases the adhesion force, but still retains the same scaling of the zero magnetic field situation.

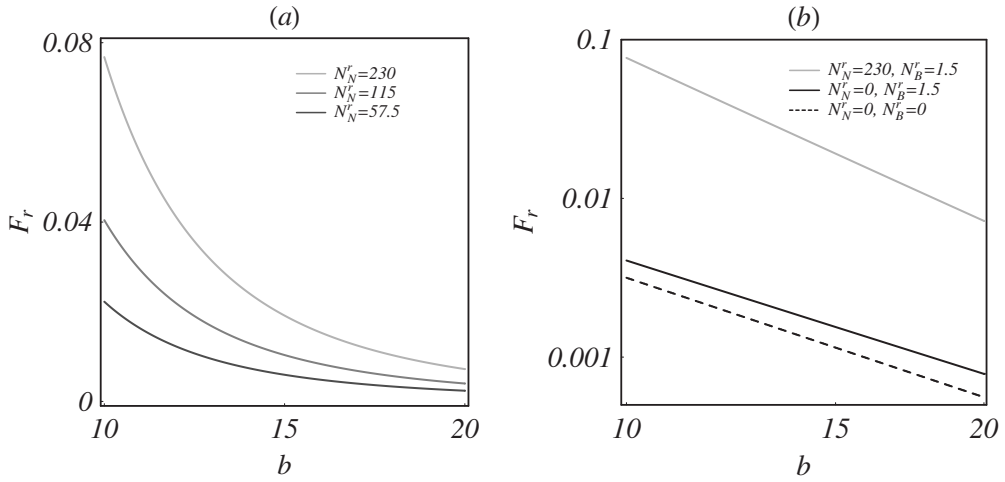

FIG. 3. Adhesion force for the radial field case F_r as a function of displacement b, for (a) $N_B^r=1.5$ and three values of N_N^r; and (b) contrasting the case of zero applied field (dashed curve), with the ones assuming the action of the radial field, for a field-independent (solid black curve), and a field-dependent yield (solid gray curve) stress MR fluid. It is assumed that $b_0=10$, and $\chi=0.1$.

B. Radial magnetic field

Very recently a theoretical study [39] has proposed that simply by reversing the direction of the current in one of the Helmholtz coils ("anti-Helmholtz" arrangement [40]), one could produce a very simple, but innovative nonuniform magnetic field disposition, given by

$$\mathbf{H}_a = \frac{H_0}{L} r\hat{\mathbf{r}} \tag{12}$$

at $z=0$, where L is a characteristic length, and $\hat{\mathbf{r}}$ represents the unit vector along the radial direction. This purely radial magnetic field acts in the mid-plane between the coils, and its real world existence has been already checked experimentally [34]. For this particular field configuration, the magnetic pressure given by Eq. (4) can be readily written as

$$\Psi_r(r) = \frac{\mu_0 \chi H_0^2 r^2}{2L^2}. \tag{13}$$

Notice that the radial applied field naturally presents a radial gradient, so that at lowest order in the magnetic force we can neglect the demagnetizing field contribution.

Before proceeding with the calculation of the adhesion force, it is worth mentioning that due to the fully three-dimensional divergence-free condition $\nabla \cdot \mathbf{H_a}=0$, near the $x-y$ plane we actually have magnetic field contributions along the radial (H_a^r) and axial (H_a^z) directions. Under the circumstances that the radius of the coils is much larger than the dimension of the MR fluid sample, we have found that

$$\frac{H_a^r}{H_a^z} = -\frac{1}{2}\frac{r}{z}. \tag{14}$$

Therefore, for the large aspect ratio situation $[R(t) \gg b(t)]$ occurring under probe-tack tests we can say that $H_a^r \gg H_a^z$. Consequently, the applied field can be considered simply as radial. Moreover, for this situation we have verified that the axial field contribution for the adhesion force is indeed much smaller [$\sim 10^2-10^3$ times smaller] than its radial counterpart.

By taken into account the discussion above, and by substituting Eq. (13) into Eq. (6) we obtain the *dimensionless* adhesion force

$$F_r = \frac{1}{b^{5/2}} + N_N^r \frac{1}{b^{7/2}} + N_B^r \chi \left(\chi + \frac{1}{2}\right)\frac{1}{b^2}, \tag{15}$$

where $N_B^r=(\pi\mu_0 H_0^2 R_0^4 b_0^2)/2k\zeta^3 L^2$ is the magnetic Bond number in the radial field case, and $N_N^r=(3\alpha H_0^2 R_0^2 b_0)/5\sigma_{y0}\zeta L^2$ is the non-Newtonian parameter. We stress that the radial adhesion force is made dimensionless by using the same rescaling utilized in the perpendicular field case.

Figure 3 depicts the force-distance curves for the radial field case, assuming that $b_0=10$, and $\chi=0.1$. Figure 3(a) considers a fixed value of $N_B^r=1.5$, and three different values of N_N^r: 230 (light gray curve), 115 (medium gray curve), and 57.5 (dark gray curve). Similarly to what has been discussed in the perpendicular field case [Fig. 2(a)] here we observe that by increasing the value of the non-Newtonian parameter N_N^r an increasingly larger adhesion force results. We point out that the similarity of behaviors shown in Figs. 2(a) and 3(a) occurs despite the differences in the symmetry properties of these magnetic field arrangements.

Figure 3(b) illustrates a log-log plot of the force-distance curves, where the lifting occurs for three distinct situations: (i) field-dependent yield stress MR fluid under the influence of a radial field ($N_N^r=230$, $N_B^r=1.5$, solid gray curve)); (ii) field-independent yield stress MR fluid under the influence of a radial field ($N_N^r=0$, $N_B^r=1.5$, solid black curve)); and (iii) MR fluid in the absence of an applied magnetic field, or "off" state MR fluid ($N_N^r=0$, $N_B^r=0$, dashed curve). In contrast to the perpendicular field case, in Fig. 3(b) we notice that the sole action of the radial field produces an increase of roughly 28% in the adhesion force with respect to the nonmagnetic situation. The origin of this behavior can be justified by the existence of an inherent field gradient along the outward radial direction, which tends to spread out the fluid droplet, making the lifting process more difficult.

Once again we verify that adhesion force is hugely increased for the case of the field-dependent yield stress MR fluid, as illustrated by the gray curve in Fig. 3(b). In this radial case the adhesion force is about 23 times larger than the one calculated for the nonmagnetic situation (dashed curve). This makes evident the great significance of the the yield stress field dependence in determining the adhesion behavior in MR fluids for both the radial and perpendicular field setups.

We conclude this section by briefly discussing the specific form of the force displacement curves under the radial magnetic field configuration shown in Fig. 3(b). As expected we observe from Eq. (15) that for the zero applied field case ($N_N^r = N_B^r = 0$) $F_r \sim b^{-5/2}$, corresponding to the dashed line. On the other hand, the contribution of the magnetic field ($N_N^r = 0$ and $N_B^r \neq 0$) related to the solid black curve introduces an additional b^{-2} dependence, which will be dominant for larger values of b. As commented earlier this happens due to the intrinsic gradient provided by the applied magnetic field. Finally, since $N_N^r \gg N_B^r$ the consideration of the field-induced yield stress adds a substantial modification on the behavior of the adhesion force, making it to vary according to $F_r \sim b^{-7/2}$ (solid gray curve). So, the field-dependent yield stress leads to a more significant drop of F_r with b as compared to the zero applied field case. Physically, this could be expected from the very nature of the radial magnetic field: due to volume conservation as b is increased the droplet contracts, and moves toward regions of lower magnetic field intensity, leading to a stronger decrease in the yield stress value. It is worth noting that the influence of the field-dependent yield stress is twofold: it hugely increases the magnitude of F_r, and also modifies its dependence on b.

IV. CONCLUDING REMARKS

One of the most desirable properties for an ideal adhesive material would be the capability of switching its adhesive strength on and off in a reversible way via an external controlling mechanism. In this work, we exploited this possibility by examining a confined plate-plate system in which a magnetorheological fluid behaves as such "smart" adhesive, when subjected to an external magnetic field. By employing a Darcy-like law approach, and considering an explicit magnetic field dependence of the yield stress, we have been able to evaluate the adhesion performance of the MR fluid. Two magnetic field configurations have been considered by using basically the same Helmholtz coils arrangement, where either a uniform perpendicular field, or a nonuniform radial field can be generated. Our analytical calculations indicate that for both field configurations one obtains adhesive forces which can be dramatically larger than the ones measured by usual situations in which field-dependent yield stress effects are not taken into account. While both field configurations lead to an enhanced adhesion force, we have detected that they behave differently regarding their scaling with respect to the plate separation b: if on one hand the perpendicular field keeps the same scaling as the zero-field case ($F_\perp \sim b^{-5/2}$), on the other hand the radial field introduces a distinct scaling where $F_r \sim b^{-7/2}$.

It is worthwhile to note that mechanisms of magnetically enhanced adhesion have been previously investigated for Newtonian [7], and non-Netonian ferrofluids [12]. Nevertheless, the increase in adhesion calculated for these systems is quite modest in comparison with the order-of-magnitude differences we have predicted in this work for magnetorheological fluids.

We point out that our theoretical results have not yet been verified by experiments. An interesting experiment on the investigation of adhesive properties of MR fluids have been recently performed by Ewoldt *et al.* [11,30] who studied the action of an inhomogeneous magnetic field produced by a small cylindrical magnet. However, considering the relative simplicity of the Helmholtz coils experimental setup we hope that experimentalists will feel motivated to check our theoretical predictions. Of course, our analytical model is an initial attempt to get some insight about the potential use of MR fluids as "smart" adhesives so that more complicated effects like cavitation and wetting failure have not been considered. Again, we expect that theorists will be inclined to add these contributions into more sophisticated theoretical descriptions of the system in the future.

ACKNOWLEDGMENTS

We thank CNPq (Brazilian Research Council) for financial support of this research through the program "Instituto Nacional de Ciência e Tecnologia de Fluidos Complexos (INCT-FCx)" and also through the CNPq/FAPESQ Pronex program.

[1] B. A. Francis and R. G. Horn, J. Appl. Phys. **89**, 4167 (2001).
[2] D. Derks, A. Lindner, C. Creton, and D. Bonn, J. Appl. Phys. **93**, 1557 (2003).
[3] M. Tirumkudulu, W. B. Russel, and T. J. Huang, Phys. Fluids **15**, 1588 (2003).
[4] S. Poivet, F. Nallet, C. Gay, and P. Fabre, Europhys. Lett. **62**, 244 (2003).
[5] S. Poivet, F. Nallet, C. Gay, J. Teisseire, and P. Fabre, Eur. Phys. J. E **15**, 97 (2004).
[6] J. A. Miranda, Phys. Rev. E **69**, 016311 (2004).
[7] J. A. Miranda, R. M. Oliveira, and D. P. Jackson, Phys. Rev. E **70**, 036311 (2004).
[8] M. Ben Amar and D. Bonn, Physica D **209**, 1 (2005).
[9] A. Lindner, D. Derks, and M. J. Shelley, Phys. Fluids **17**, 072107 (2005).
[10] J. Nase, A. Lindner, and C. Creton, Phys. Rev. Lett. **101**, 074503 (2008).
[11] R. Ewoldt, G. McKinley, and A. Hosoi, Bull. Am. Phys. Soc. **53**(15), 252 (2008).
[12] S. A. Lira and J. A. Miranda, Phys. Rev. E **79**, 046303 (2009).
[13] A. Zosel, Colloid Polym. Sci. **263**, 541 (1985).
[14] H. Lakrout, P. Sergot, and C. Creton, J. Adhes. **69**, 307 (1999).
[15] R. E. Rosensweig, *Ferrohydrodynamics* (Cambridge University Press, Cambridge, 1985).

[16] E. Blums, A. Cebers, and M. M. Maiorov, *Magnetic Fluids* (de Gruyter, New York, 1997).
[17] S. Odenbach, J. Phys.: Condens. Matter **16**, R1135 (2004); L. M. Pop and S. Odendach, *ibid.* **18**, S2785 (2006).
[18] S. Odenbach, L. M. Pop, and A. Y. Zubarev, GAMM-Mitteilungen **30**, 195 (2007).
[19] H. Shahnazian and S. Odenbach, Int. J. Mod. Phys. B **21**, 4806 (2007).
[20] H. Shahnazian and S. Odenbach, J. Phys.: Condens. Matter **20**, 204137 (2008).
[21] H. A. Barnes, J. Non-Newtonian Fluid Mech. **81**, 133 (1999).
[22] J. Rabinow, AIEE Trans. **67**, 1308 (1948).
[23] J. M. Ginder, in *Encyclopedia of Applied Physics*, edited by G. L. Trigg (VCH, Weinheim, 1996), Vol. 16, p. 487.
[24] J. M. Ginder, MRS Bull. **23**, 26 (1998).
[25] G. Bossis, S. Lacis, A. Meunier, and O. Volkova, J. Magn. Magn. Mater. **252**, 224 (2002).
[26] S. Genç and P. P. Phulé, Smart Mater. Struct. **11**, 140 (2002).
[27] P. Coussot, J. Fluid Mech. **380**, 363 (1999).
[28] G. H. Covey and B. R. Stanmore, J. Non-Newtonian Fluid Mech. **8**, 249 (1981).
[29] A. Lindner, P. Coussot, and D. Bonn, Phys. Rev. Lett. **85**, 314 (2000).
[30] R. Ewoldt, Ph.D. thesis, Massachusetts Institute of Technology, 2009.
[31] D. P. Jackson, R. E. Goldstein, and A. O. Cebers, Phys. Rev. E **50**, 298 (1994).
[32] A. O. Cebers, Magnetohydrodynamics **17**, 113 (1981).
[33] M. Igonin, Ph.D. thesis, University Paris 7 and University of Latvia, 2004.
[34] C.-Y. Chen, Y.-S. Yang, and J. A. Miranda, Phys. Rev. E **80**, 016314 (2009).
[35] P. Kuzhir, M. T. López-López, and G. Bossis, Phys. Fluids **21**, 053101 (2009).
[36] P. P. Phulé and J. M. Ginder, Int. J. Mod. Phys. B **13**, 2019 (1999).
[37] S. A. Langer, R. E. Goldstein, and D. P. Jackson, Phys. Rev. A **46**, 4894 (1992).
[38] R. Ewoldt, G. McKinley, and A. Hosoi (private communication).
[39] R. M. Oliveira, J. A. Miranda, and E. S. G. Leandro, Phys. Rev. E **77**, 016304 (2008).
[40] T. H. Bergeman, G. Erez, and H. J. Metcalf, Phys. Rev. A **35**, 1535 (1987).